

Cosmological viable models in $f(T,B)$ gravity as solutions to the H_0 tension

Celia Escamilla-Rivera^{*}

*Instituto de Ciencias Nucleares, Universidad Nacional Autónoma de México,
Circuito Exterior C.U., A.P. 70-543, México D.F. 04510, México.*

Jackson Levi Said[†]

*Institute of Space Sciences and Astronomy, University of Malta, Msida, MSD 2080, Malta and
Department of Physics, University of Malta, Msida, MSD 2080, Malta*

In this work we present a further investigation about Teleparallel Gravity Cosmology. We demonstrate that according the current astrophysical data (CC+Pantheon+BAO samplers with late universe measurements SH0ES+H0LiCOW), a $f(T,B)$ theory can provide another interpretation to the oscillatory behaviour of the dark energy equation of state when applied to late times. The four $f(T,B)$ cosmological viable models proposed here can undergo an epoch of late-time acceleration and reproduce quintessence and phantom regimes with a transition along the phantom-divided line, making this theory a good approach to modify the standard Λ CDM model.

I. INTRODUCTION

It is well known that the Λ CDM cosmological model is motivated by astounding success in describing the Universe at all scales where observations can be made [1, 2]. Through the proposal of cold dark matter, this cosmological model can adequately describe the dynamics of galaxies, and through the effects of dark energy: the cosmic acceleration of the Universe [3, 4]. However, despite great efforts, dark matter remains undetected and the cosmological constant description via dark energy continues to have numerous problems associated with it [5].

On one hand, recently, the effectiveness of the Λ CDM model in explaining precision cosmology observations has been called into question. This is primarily through the so-called H_0 tension problem which is a discrepancy between the predicted value of H_0 from the early Universe and its observed value from the local measurements. First reported as a serious tension by the Planck collaboration in [6, 7], the tension has since grown by means of strong lensing measurements from the H0LiCOW (H_0 lenses in Cosmograil's wellspring) collaboration [8] and from Cepheids via SH0ES (Supernovae H_0 for equation of state) [9]. Meanwhile, measurements based on the tip of the red giant branch (TRGB, Carnegie-Chicago Hubble Program) have yielded a lower H_0 tension [10]. There also exist novel methods of determining the value of H_0 through gravitational wave astronomy [11, 12] that may shed light in the problem.

On the other hand, by construction, Λ CDM is based on taking Einstein's theory of General Relativity (GR) and modifying the matter content part of the theory to satisfy observational demands. However, it may also be the case that the gravity content of the cosmological model needs to be corrected for these observational scales. There have been a plethora of theories that have been proposed which have had varying success in explaining the Universe. However, by and large these theories mainly rely on considering gravity GR through the prism of the Levi-Civita connection which expresses gravitation through the curvature of spacetime. In this work, we consider Teleparallel Gravity (TP) which differs from GR in that it manifests gravity through torsion rather than curvature [13], which is achieved by replacing the Levi-Civita connection with the Weitzenböck connection. At the level of the gravitational action, GR and TG can be made to be equal up to a boundary term, this is the so-called *Teleparallel equivalent of General Relativity* (TEGR). Straightforwardly, TEGR will produce the same field equations as GR, but the ensuing modifications that can be constructed will naturally be distinct. TG also has a number of other advantageous features such as its similarity to Yang-mills theory [14] giving it an added particle physics dimension. It is also possible to define a gravitational energy-momentum tensor in TG [15, 16] which means separating inertia and gravitation. TG is more regular than GR in that it does not require the introduction of a Gibbons–Hawking–York boundary term when in order to produce a well-defined Hamiltonian formulation [17]. Even more, TG is an interesting theory of gravity since it does not necessarily require the equivalence principle to hold, that is, unlike GR where this is a fixed feature, TG would survive a violation of this principle [18].

As with GR, TG can be readily modified in numerous routes: the TEGR Lagrange density is the so-called torsion scalar T (discussed in §. II), where we can immediately generalise to $f(T)$ theory which has generally second-order

^{*}Electronic address: celia.escamilla@nucleares.unam.mx

[†]Electronic address: jackson.said@um.edu.mt

field equations unlike $f(R)$ gravity [19–21] that is a fourth-order theory. Many of the same analyses that occur in Levi-Civita based theories of gravity can be analogously constructed in TG. However, given the ease of constructing second-order theories in TG means that there are modified theories of gravity in the TG framework that do not exist in curvature-based models of gravity. One such example is $f(T, B)$ theory where B is the boundary term between the torsion and Ricci scalars [22–27, 27, 28]. This model decouples the second- and fourth-order contributions in models of gravity contains $f(R)$ gravity as a subset. This is a more *natural way* of studying the contributions of $f(R)$ gravity.

Therefore, if we choose to work with TG in a specific class of cosmological frames we need to consider a flat FRW background metric with a tetrad depending of the scale factor and a vanishing spin connection. In this scenario, this choice is the exact solution of the teleparallel version of the gravitational field equation and it can be seen that the corresponding Friedmann equations are identical to the GR ones [29]. As an extension of this landscape, we can introduce scalar fields as source of dark energy in the case of minimal coupling, e.g quintessence field [30], unlike in the non-minimal case, where the scale factor sector is coupled to gravity, with the torsion scalar in TG and the curvature scalar in GR. In analogy to this line of thought, in this work we propose four forms of $f(T, B)$ models in order to study the late cosmological dynamics and see that we can mimic the same effect of dark energy and solve the current H_0 tension in some scenarios.

Throughout this work, Latin indices are used to refer to coordinates on the tangent space, while Greek indices refer to general manifold coordinates. Also, the metric signature is $\eta_{\mu\nu} = \text{diag}(-1, 1, 1, 1)$. The outline of the paper is as follows: in §. II we describe the TG background theory in order to set the equivalence with GR. In §. III we explore a flat homogeneous and isotropic cosmology in the $f(T, B)$ gravity setting in order to derive a generic equation of state for the theory. In §. IV, we describe the observational data being used to constrain the cosmological parameters for the models being investigated. §. V contains the analyses of the $f(T, B)$ models being proposed. The observational constraints will be obtained using astrophysical data as galaxy ages sampler, BAO samples and supernovae Type Ia current sampler (Pantheon). The statistical results are shown for each model. Finally, a summary and conclusion of our work is given in §. VI. An Appendix with all the general calculations for each proposed cosmological model can be found at the end.

II. TELEPARALLEL GRAVITY BACKGROUND

General Relativity (GR) expresses gravitation in terms of curvature by means of the Levi-Civita connection, $\overset{\circ}{\Gamma}{}^\sigma{}_{\mu\nu}$ [1]. However, Riemann geometry contains other means of geometric deformation which can be used to describe gravity. In fact, there exists a trinity of characterizations of gravity such that GR can be reproduced at the level of the field equations in a particular limit [31]. In this work, we consider the setting of TG [17, 32, 33]. TG is fundamentally distinct from curvature-based descriptions of gravity in that the Levi-Civita connection is replaced with the Weitzenböck connection, $\Gamma^\sigma{}_{\mu\nu}$, which is a curvatureless connection that observes the metricity condition [13, 14]. The Weitzenböck connection is defined by

$$\Gamma^\sigma{}_{\mu\nu} := e_a{}^\sigma \partial_\mu e^a{}_\nu + e_a{}^\sigma \omega^a{}_{b\mu} e^b{}_\nu, \quad (1)$$

where $e^a{}_\rho$ is the tetrad field ($e_a{}^\mu$ being the transpose), and $\omega^a{}_{b\mu}$ the spin connection. This is the most general linear affine connection that is both curvatureless and satisfies the metricity condition [32]. The tetrad relates the general manifold and the tangent (inertial) space, represented by the inertial Latin indices and the general manifold Greek indices. On the other hand, the spin connection appears in order to conserve the invariance of teleparallel theories under Local Lorentz Transformations (LLT) [34]. Thus, the spin connection incorporates the LLT freedom for any choice of theory based on the Weitzenböck connection. GR also has an associated spin connection, but this is mainly hidden in the inertial structure of the theory [32]. Together, the tetrad and its associated spin connection play the same role as the metric tensor in curvature-based theories of gravity.

The spin connection can be determined by considering the the full breath of LLTs (Lorentz boosts and rotations), where the tetrad is transformed by its inertial index through

$$e'^a{}_\mu = \Lambda^a{}_b e^b{}_\mu, \quad (2)$$

where $\Lambda^a{}_b$ is a LLT. The spin connection can then be represented as the combination of completely inertial LLTs in the form [35]

$$\omega^a{}_{b\mu} = \Lambda^a{}_c \partial_\mu \Lambda_b{}^c, \quad (3)$$

which preserves the LLT invariance of the theory as a whole. However, there also exist so-called good tetrad choices which produce vanishing spin connection components [36, 37]. Given the invariance of the theory under LLTs, all consistent tetrad and spin connection choices will be dynamically equivalent.

As it was mentioned, the metric tensor, $g_{\mu\nu}$, expresses geometric deformation through distance measurements, while the tetrad, e^a_μ relates the tangent space with the general manifold. For consistency, they also observe the relations [14]

$$e^a_\mu e_b^\mu = \delta_b^a, \quad e^a_\mu e_a^\nu = \delta_\mu^\nu, \quad (4)$$

which form the orthogonality conditions of the tetrad fields. Naturally, the tetrad fields can be used to transform between the inertial Minkowski metric and a general manifold through

$$g_{\mu\nu} = e^a_\mu e_b^\nu \eta_{ab}, \quad \eta_{ab} = e_a^\mu e_b^\nu g_{\mu\nu}, \quad (5)$$

where the tetrad can be seen to replace the metric tensor as the fundamental dynamical object of the theory. The position dependence of these relations is being suppressed for brevity's sake. One important point is that the curvature measured by the Riemann tensor will always vanish in TG because the Weitzenböck connection is curvatureless, while the torsion will depend on the specific form of the tetrad and its associated spin connection. In this scenario, torsion is represented by the anti-symmetric part [37]

$$T^\sigma_{\mu\nu} := 2\Gamma^\sigma_{[\mu\nu]}, \quad (6)$$

which is a measure of the field strength of gravitation, and where square brackets represent the anti-symmetric operator ($A_{[\mu\nu]} = \frac{1}{2}(A_{\mu\nu} - A_{\nu\mu})$). $T^\sigma_{\mu\nu}$ is called the torsion tensor and transforms covariantly under both diffeomorphisms and LLTs. Analogous to the Riemann tensor, the torsion tensor is a measure of torsion for a gravitational field. However, other useful tensors can also be defined, such as the contorsion tensor which is the difference between the Levi-Civita and Weitzenböck connections [17, 38]

$$K^\sigma_{\mu\nu} := \Gamma^\sigma_{\mu\nu} - \mathring{\Gamma}^\sigma_{\mu\nu} = \frac{1}{2}(T_\mu^\sigma{}_\nu + T_\nu^\sigma{}_\mu - T^\sigma_{\mu\nu}). \quad (7)$$

Naturally, this plays a crucial role in relating TG with Levi-Civita based theories. Another important ingredient in forming a teleparallel theory of gravity is the so-called superpotential which is defined as

$$S_a^{\mu\nu} := K^{\mu\nu}{}_a - h_a{}^\nu T^{\alpha\mu}{}_\alpha + h_a{}^\mu T^{\alpha\nu}{}_\alpha. \quad (8)$$

The superpotential plays an important role in representing TG as a gauge current for a gravitational energy-momentum tensor [39]. Contracting the torsion and superpotential tensors, the so-called torsion scalar is produced through

$$T := S_a^{\mu\nu} T^\alpha_{\mu\nu}, \quad (9)$$

which is determined solely by the Weitzenböck connection but can be used to compare with results with standard gravity. Coincidentally, it turns out that the torsion and Ricci scalars are equal up to a total divergence term [22, 40], namely

$$R = \mathring{R} + T - \frac{2}{e} \partial_\mu (e T^\sigma{}_\sigma{}^\mu) = 0 \quad \Rightarrow \quad \mathring{R} = -T + \frac{2}{e} \partial_\mu (e T^\sigma{}_\sigma{}^\mu) := -T + B, \quad (10)$$

where \mathring{R} is the Ricci scalar as determined using the Levi-Civita connection, R is the Ricci scalar as calculated with the Weitzenböck connection which vanishes, and e is the determinant of the tetrad field, $e = \det(e^a_\mu) = \sqrt{-g}$. This relation alone guarantees that the torsion and Ricci scalars produce the same dynamical equations. Also, this means that the second and fourth order contributions to the Ricci scalar can be decoupled in TG. This may have important consequences for providing a more natural generalization of $f(R)$ gravity [23].

One straightforward result of this equivalency is that we can define TEGR as [37]

$$\mathcal{S}_{\text{TEGR}} = -\frac{1}{2\kappa^2} \int d^4x e T + \int d^4x e \mathcal{L}_m, \quad (11)$$

where $\kappa^2 = 8\pi G$, and \mathcal{L}_m represents the Lagrangian for matter. Consequently, TEGR will produce identical Einstein field equations

$$\mathring{G}_{\mu\nu} \equiv e^{-1} e^a_\mu g_{\nu\rho} \partial_\sigma (e S_a^{\rho\sigma}) - S_b^\sigma{}_\nu T^b{}_{\sigma\mu} + \frac{1}{4} T g_{\mu\nu} - e^a_\mu \omega^b{}_{a\sigma} S_{b\nu}{}^\sigma = \kappa^2 \Theta_{\mu\nu}, \quad (12)$$

where $\Theta_{\mu\nu}$ is the energy-momentum tensor [1], and $\mathring{G}_{\mu\nu}$ is the Einstein tensor calculated with the Levi-Civita connection.

Similar to the $f(\mathring{R})$ generalization of GR [20, 23], the TEGR Lagrangian density can be generalized to $f(T)$ gravity [41–45]. This produces second order field equations [17], as well as a number similarities to GR such as exhibiting the same gravitational wave polarizations [26]. However, to incorporate both the second and fourth order components of $f(\mathring{R})$, it is advantageous to consider $f(T, B)$ gravity which forms a larger class of theories than those expressed through $f(\mathring{R})$ gravity (at the level of field equations) [22–27, 27, 28]. By generalizing $f(\mathring{R})$ gravity in terms of its order contributions, $f(T, B)$ gravity may provide an interesting avenue to study fourth order modified theories of gravity.

III. F(T,B) COSMOLOGY

To explore the cosmology that emerges from $f(T, B)$ gravity, we consider a flat homogeneous and isotropic metric as FLRW. We choose to take this in Cartesian coordinates so that the metric takes the form

$$ds^2 = -dt^2 + a(t)^2(dx^2 + dy^2 + dz^2), \quad (13)$$

where $a(t)$ is the scale factor, and the lapse function is already set to unity. This can be done since $f(T, B)$ gravity retains diffeomorphism invariance. By taking the choice of tetrad as [33]

$$h^a{}_\mu = \text{diag}(1, a(t), a(t), a(t)), \quad (14)$$

the spin connection components turn out to all be zero, i.e. $\omega^a{}_{b\mu} = 0$ [24]. There exist an infinite number of possible choices for the tetrad which satisfy (5) but only a small subset are good tetrads, i.e. have vanishing associated spin connections. For this spacetime, the torsion scalar is explicitly given by

$$T = 6H^2, \quad (15)$$

while the boundary term is given by

$$B = 6 \left(3H^2 + \dot{H} \right). \quad (16)$$

Together, these form the Ricci scalar through the relation in (10), that is

$$\mathring{R} = -T + B = 6 \left(\dot{H} + 2H^2 \right), \quad (17)$$

is recovered. This shows how $f(\mathring{R})$ gravity results as a subset of $f(T, B)$ gravity where

$$f(T, B) := f(-T + B) = f(\mathring{R}), \quad (18)$$

which only represents a small part of the space of models in $f(T, B)$ gravity. Also, the respectively second and fourth order natures of the torsion scalar and boundary term can be appreciated through this choice of tetrad.

Evaluating the field equations for a Universe filled with a perfect fluid, the Friedmann equations turn out to be given by [24, 27]

$$-3H^2(3f_B + 2f_T) + 3H\dot{f}_B - 3\dot{H}f_B + \frac{1}{2}f = \kappa^2\rho_m, \quad (19)$$

$$-\left(3H^2 + \dot{H}\right)(3f_B + 2f_T) - 2H\dot{f}_T + \ddot{f}_B + \frac{1}{2}f = -\kappa^2 p_m, \quad (20)$$

where ρ_m and p_m represent the energy density and pressure of the matter content respectively. On taking the arbitrary Lagrangian mapping

$$f(T, B) \rightarrow -T + f(T, B), \quad (21)$$

the field equations can be re-expressed as

$$3H^2 = \kappa^2(\rho_m + \rho_{\text{eff}}), \quad (22)$$

$$3H^2 + \dot{H} = -\kappa^2(p_m + p_{\text{eff}}), \quad (23)$$

where the modified TEGR components are contained in the effective fluid contributions given as

$$\kappa^2 \rho_{\text{eff}} = 3H^2 (3f_B + 2f_T) - 3H\dot{f}_B + 3\dot{H}f_B - \frac{1}{2}f, \quad (24)$$

$$\kappa^2 p_{\text{eff}} = \frac{1}{2}f - \left(3H^2 + \dot{H}\right) (3f_B + 2f_T) - 2H\dot{f}_T + \ddot{f}_B, \quad (25)$$

which can be combined to give

$$2\dot{H} = -\kappa^2 (\rho_m + p_m + \rho_{\text{eff}} + p_{\text{eff}}). \quad (26)$$

The effective fluid that acts as the modified part of the $f(T, B)$ Lagrangian turns out to also satisfy the conservation equation

$$\dot{\rho}_{\text{eff}} + 3H(\rho_{\text{eff}} + p_{\text{eff}}) = 0. \quad (27)$$

Finally, an equation of state (EoS) can be written for this effective fluid as

$$w_{\text{eff}} = \frac{p_{\text{eff}}}{\rho_{\text{eff}}} \quad (28)$$

$$= -1 + \frac{\ddot{f}_B - 3H\dot{f}_B - 2\dot{H}f_T - 2H\dot{f}_T}{3H^2 (3f_B + 2f_T) - 3H\dot{f}_B + 3\dot{H}f_B - \frac{1}{2}f}. \quad (29)$$

Notice that we can recover the standard Λ CDM case ($w_{\text{eff}} = -1$) when we switch off the T and B terms. Since the latter equation is linked to a specific form of $f(T, B)$, in this work we consider four cosmological models in order to investigate the possibility the effects of a late acceleration cosmic expansion without the influence of a exotic dark energy or extra fields. It is important to remark that, in comparison to [17], we solve the entire full system of equations (15)-(16) and the corresponding cosmological model.

IV. CURRENT OBSERVATIONAL DATA

Given that we are interested in modelling the late-time evolution of the Universe, we use observational data from SNeIA luminosity distance from Pantheon compilation and BAO redshift surveys [46] and the high- z measurements of $H(z)$ from Galaxy ages (CC) [47].

In order to carry out cosmological tests for the free parameters of each of the $f(T, B)$ models proposed below, we are going to consider the constraints solutions over T and B imposed by each case and determine the specific cosmological parameters for each model in addition to Ω_m and H_0 late Universe data. We use the publicly codes CLASS¹ and Monte Python² to constrain the models using a total sampler of CC+SNeIa+BAO.

Figures 2-4-6-8 show the parameter space for w_{model} and Ω_m with their probability density function (PDF) versus Ω_m up to 3- σ confidences levels (CL) using the joint sampler CC+Pantheon+BAO.

A. Galaxy ages

Given that distance scale measurements require integrals of $H(z)$, it is a standard point of view that it is more precise to study the observational $H(z)$ data directly rather than these means since information loses are a natural consequence of these integrals, and of course, the errors that these can carry out. As an independent approach of this measure we provide the Cosmic Chronometers (CC) sample. This kind of sample gives a measurement of the expansion rate without relying on the nature of the metric between the chronometer and us. A full compilation of the latter, which includes 38 measurements of $H(z)$ in the range $0.07 < z < 2.36$ are reported in [47].

¹ https://github.com/lesgourg/class_public

² https://github.com/naudren/montepython_public

B. Pantheon Type Ia supernovae compilation

This sample consists of 40 bins [46] compressed. Notice that, since we are performing an EoS that at some point recover Λ CDM, the binned catalog is not a problem in the sense of favoring this model. Type Ia supernovae can give determinations of the distance modulus μ , whose theoretical prediction is related to the luminosity distance d_L according to

$$\mu(z) = 5 \ln \left[\frac{d_L(z)}{1 \text{Mpc}} \right] + 25, \quad (30)$$

where the luminosity distance is given in Mpc. In the standard statistical analysis, one adds to the distance modulus the nuisance parameter M , an unknown offset sum of the supernovae absolute magnitude (and other possible systematics), which is degenerate with H_0 . As we are assuming spatial flatness, the luminosity distance is related to the comoving distance D via

$$d_L(z) = \frac{c}{H_0} (1+z) D(z), \quad (31)$$

where c is the speed of light, so that, using Eq.(30), we can obtain

$$D(z) = \frac{H_0}{c} (1+z)^{-1} 10^{\frac{\mu(z)}{5} - 5}. \quad (32)$$

Therefore, the normalised Hubble function $H(z)/H_0$ can be obtained by taking the inverse of the derivative of $D(z)$ with respect to the redshift $D(z) = \int_0^z H_0 d\tilde{z}/H(\tilde{z})$. Since we are taking nuisance parameter M in the sample, we choose the respective values of M from a statistical analysis of the Λ CDM model with the Pantheon sample obtained by fixing H_0 to the Planck value in Eq.(33) with TT, TE, EE + lowE + lensing +BAO and to the Late Universe measurements as

$$H_0 = 67.4 \pm 0.5 \text{km/s/Mpc}, \quad \text{from Planck 2018}, \quad (33)$$

$$H_0 = 73.8 \pm 1.1 \text{km/s/Mpc}, \quad \text{from Late Universe (SH0ES + H0LiCOW)}, \quad (34)$$

To perform this we have used a Monte Python code and obtained $M = -19.63$ for Planck 2018 and $M = -32.79$ for SH0ES+H0LiCOW.

C. BAO samples

We also consider in our analysis the measurements of BAO observations in the galaxy distribution. These observations can contribute important features by comparing the data of the sound horizon today to the sound horizon at the time of recombination (extracted from the CMB anisotropy data). Commonly, the BAO distances are given as a combination of the angular scale and the redshift separation: $d_z \equiv \frac{r_s(z_d)}{D_V(z)}$, with $r_s(z_d) = \frac{c}{H_0} \int_{z_d}^{\infty} \frac{c_s(z)}{E(z)} dz$ and $r_s(z_d)$ being the comoving sound horizon at the baryon dragging epoch, c the light velocity, z_d is the drag epoch redshift and $c_s^2 = c^2/3[1 + (3\Omega_{b0}/4\Omega_{\gamma0})(1+z)^{-1}]$ the sound speed with Ω_{b0} and $\Omega_{\gamma0}$ the present values of baryon and photon density parameters, respectively. By definition, the dilation scale is

$$D_V(z, \Omega_m; w_0, w_1) = \left[(1+z)^2 D_A^2 \frac{c z}{H(z, \Omega_m; w_0, w_1)} \right]^{1/3}, \quad (35)$$

where D_A is the angular diameter distance

$$D_A(z, \Omega_m; w_0, w_1) = \frac{1}{1+z} \int_0^z \frac{c d\tilde{z}}{H(\tilde{z}, \Omega_m; w_0, w_1)}. \quad (36)$$

Through the comoving sound horizon, the distance ratio d_z is related to the expansion parameter h (defined such that $H \doteq 100h$) and the physical densities Ω_m and Ω_b . We use measurements of the BAO peak from the galaxy redshift surveys six-degree-field galaxy survey (6dFGS, Sloan Digital Sky Survey Data Release 7 (SDSS DR7) and the reconstructed value (SDSS(R)), as well as the latest result from the complete BOSS sample SDSS DR12, and also from the Lyman- α Forest measurements from the Baryon Oscillation Spectroscopic Data Release 11 (BOSS DR11). Since the volume surveyed by BOSS and WiggleZ [48] partially overlap we do not use data from the latter in this work (see details in Ref.[49]). The total χ_{BAO}^2 is directly obtained by the sum of the individual quantity: $\chi_{\text{BAO-total}}^2 = \chi_{\text{6dFGS}}^2 + \chi_{\text{SDSS}}^2 + \chi_{\text{BOSS}}^2 + \chi_{\text{Ly}\alpha\text{-F}}^2$. The full sampler of these data is shown in Table I.

Data set	z	$r_{\text{BAO}}(z)$
6dF	0.106 [50]	0.336 ± 0.015
SDSS DR7	0.15 [51]	0.2239 ± 0.0084
SDSS(R) DR7	0.35 [52]	0.1137 ± 0.0021
SDSS(R)-III DR12	0.38 [53]	0.100 ± 0.0011
	0.61 [54]	0.0691 ± 0.0007
SDSS(R)-III DR12	2.34 [55]	0.0320 ± 0.0013
	2.36 [56]	0.0329 ± 0.0009

TABLE I: $r_{\text{BAO}}(z)$ measurements used in this work. The selected ones corresponding to SDSS data were inverted from the published values of $D_V(z)/s_d$ and those corresponding to Ly α -F data were obtained from the reported quantities $D_A(z)/s_d$ and $D_H(z)/s_d$.

V. COSMOLOGICALLY INSPIRED F(T,B) MODELS

In this section we are going to consider four possible cosmological models in order to study late time cosmic accelerations and compliments this with a study of the effects of dynamical dark energy-like equation of state that each model produces.

A. General Taylor Expansion Model

As in [26], first consider a general Taylor expansion of the $f(T, B)$ Lagrangian, given as

$$f(T, B) = f(T_0, B_0) + f_T(T_0, B_0)(T - T_0) + f_B(T_0, B_0)(B - B_0) + \frac{1}{2!}f_{TT}(T_0, B_0)(T - T_0)^2 + \frac{1}{2!}f_{BB}(T_0, B_0)(B - B_0)^2 + f_{TB}(T_0, B_0)(T - T_0)(B - B_0) + \mathcal{O}(T^3, B^3), \quad (37)$$

where we need to go beyond linear approximations since B is a boundary term at linear order. For a Minkowski background, it follows that

$$T_0 = 0, \quad B_0 = 0, \quad (38)$$

but, until this point, it is not clear what the values of the arbitrary Lagrangian f will be, and so taking constants A_i , the Lagrangian can be written as

$$f(T, B) \simeq A_0 + A_1T + A_2T^2 + A_3B^2 + A_4TB, \quad (39)$$

where the linear boundary term has been removed. All the derivatives corresponding to f_T and f_B functions for this model can be found in Appendix A.

From Eq.(24) adding $3H^2$ to both sides we then write

$$H^2 = \frac{1}{2} \left[3H^2(1 - 3f_B - 2f_T) + \frac{1}{2}f + 3H\dot{f}_B - 3\dot{H}f_B \right] + \frac{\kappa^2}{3}\rho, \quad (40)$$

which can be comparing to $H^2 = \kappa^2/3(\rho + \rho_X)$, where ρ_X is denominates the X -fluid. We can define the terms in brackets as

$$\kappa^2\rho_X := 3H^2(1 - 3f_B - 2f_T) + \frac{1}{2}f + 3H\dot{f}_B - 3\dot{H}f_B, \quad (41)$$

in this way, the matter term does not appear explicitly in ρ_X . For this case, the corresponding EoS is given by ³

$$w_x(a) = \frac{-24w_{x_7}\dot{a}(t)^5 + 6a(t)^4 [\ddot{a}(t) - 4A_3a^{(4)}(t)] + 24a(t)\dot{a}(t)^3w_{x_1} - 6a(t)^3w_{x_2} + 24a(t)^2\dot{a}(t)w_{x_3} + w_{x_8}}{-6a(t)^4\ddot{a}(t) + w_{x_5} + 72a(t)\dot{a}(t)^3w_{x_4} + w_{x_6}}, \quad (42)$$

³ We represented here $a^{(i)}$, with $i > 2$ as high derivatives with respect to t .

where

$$w_{x_1} = [(4A_2 + 27A_3 + 11A_4) \ddot{a}(t) - (4A_2 + 12A_3 + 7A_4) \dot{a}(t)] , \quad (43)$$

$$w_{x_2} = \left[4(3A_3 + A_4) \ddot{a}(t)^2 + \dot{a}(t)^2 + 4a^{(3)}(t) (2A_3 \dot{a}(t) - A_4 \ddot{a}(t)) \right] , \quad (44)$$

$$w_{x_3} = \left[(9A_3 + 2A_4) a^{(3)}(t) \dot{a}(t) + \ddot{a}(t) ((4A_2 + 3A_4) \ddot{a}(t) + 2(2A_2 + 9A_3 + 4A_4) \dot{a}(t)) \right] , \quad (45)$$

$$w_{x_4} = -[(4A_2 + 9A_3 + 6A_4) \ddot{a}(t) + (4A_3 + A_4) \dot{a}(t)] , \quad (46)$$

$$w_{x_5} = 72(4A_2 + 12A_3 + 7A_4) \dot{a}(t)^5 + 6a(t)^3 \dot{a}(t) (12A_3 a^{(3)}(t) + \dot{a}(t)) , \quad (47)$$

$$w_{x_6} = 72(3A_3 + A_4) a(t)^2 \dot{a}(t)^2 [\ddot{a}(t) - a^{(3)}(t)] + a(t)^5 [A_3 B^2 + T(A_4 B + A_2 T + A_1) + A_0] , \quad (48)$$

$$w_{x_7} = 8A_2 + 36A_3 + 17A_4 , \quad (49)$$

$$w_{x_8} = a(t)^5 [- (A_3 B^2 + T(A_4 B + A_2 T + A_1) + A_0)] , \quad (50)$$

In order to perform the numerical analysis, we rewrite the above expression in terms of redshift $z = a_0/a - 1$, where $z = 0$ corresponds to the present time. The EoS of this model can be expressed as

$$w(z) = \frac{w(z)_1 + 6[w(z)_2 - w(z)_6] + 24[w(z)_3 - w(z)_4 - w(z)_5]}{-w(z)_1 - 6w(z)_7 + 72[w(z)_8 - w(z)_9 - w(z)_{10}] - \frac{12}{(z+1)^7}} , \quad (51)$$

where each $w(z)_i$ function is given by

$$w(z)_1 = -\frac{A_3 B^2 + T(A_4 B + A_2 T + A_1) + A_0}{(z+1)^5} , \quad (52)$$

$$w(z)_2 = \frac{\frac{2}{(z+1)^3} - \frac{96A_3}{(z+1)^5}}{(z+1)^4} , \quad (53)$$

$$w(z)_3 = \frac{(8A_2 + 36A_3 + 17A_4)}{(z+1)^{10}} , \quad (54)$$

$$w(z)_4 = \frac{\frac{2(4A_2 + 27A_3 + 11A_4)}{(z+1)^3} + \frac{4A_2 + 12A_3 + 7A_4}{(z+1)^2}}{(z+1)^7} , \quad (55)$$

$$w(z)_5 = \frac{\frac{6(9A_3 + 2A_4)}{(z+1)^6} + \frac{2\left(\frac{2(4A_2 + 3A_4)}{(z+1)^3} - \frac{2(2A_2 + 9A_3 + 4A_4)}{(z+1)^2}\right)}{(z+1)^3}}{(z+1)^4} , \quad (56)$$

$$w(z)_6 = \frac{\frac{16(3A_3 + A_4)}{(z+1)^6} - \frac{24\left(-\frac{2A_3}{(z+1)^2} - \frac{2A_4}{(z+1)^3}\right)}{(z+1)^4} + \frac{1}{(z+1)^4}}{(z+1)^3} , \quad (57)$$

$$w(z)_7 = -\frac{\frac{72A_3}{(z+1)^4} + \frac{1}{(z+1)^2}}{(z+1)^5} , \quad (58)$$

$$w(z)_8 = \frac{(3A_3 + A_4) \left[\frac{2}{(z+1)^3} + \frac{6}{(z+1)^4} \right]}{(z+1)^6} , \quad (59)$$

$$w(z)_9 = \frac{4A_2 + 12A_3 + 7A_4}{(z+1)^{10}} , \quad (60)$$

$$w(z)_{10} = \frac{\frac{4A_3 + A_4}{(z+1)^2} - \frac{2(4A_2 + 9A_3 + 6A_4)}{(z+1)^3}}{(z+1)^7} . \quad (61)$$

To solve the system of equations in Eqs.(15)-(16) we are going to analyse the behaviour of the (51) EoS associated with the X -fluid considering four kind of cases (c.f. Figure 1)

- Case 1.1: Solving the system Eqs.(15)-(16) with the condition that $T < B$, i.e we have domination of the boundary term over the torsion scalar. Also we consider A_i as positive values.
- Case 1.2: Solving the system Eqs.(15)-(16) with the condition that $T > B$, i.e we have domination of the torsion scalar over the boundary term). Also we consider A_i as positive values.

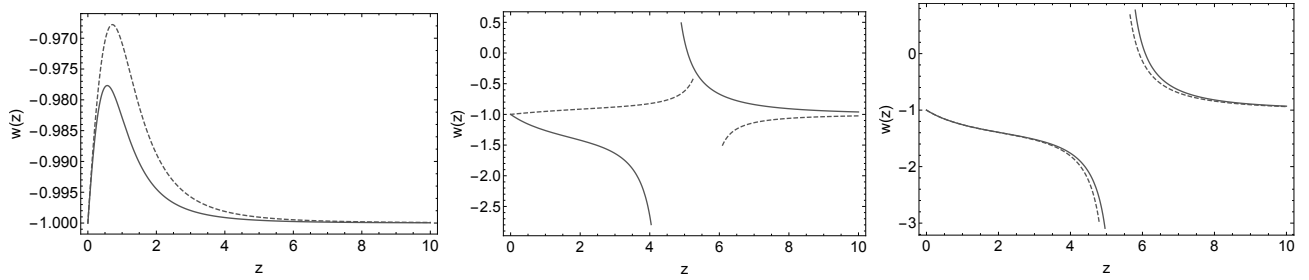


FIG. 1: Evolution of General Taylor Expansion EoS (51). *Left*: Case 1: with the condition that $T < B$ (solid line) and $T > B$ (dashed line). *Middle*: Case 2.1: $A_{i+1} > A_i$ with $T < B$ (solid line) and $T > B$ (dashed line). *Right*: Case 2.2: $A_{i+1} > A_i$ with $T < B$ (solid line) and $T > B$ (dashed line).

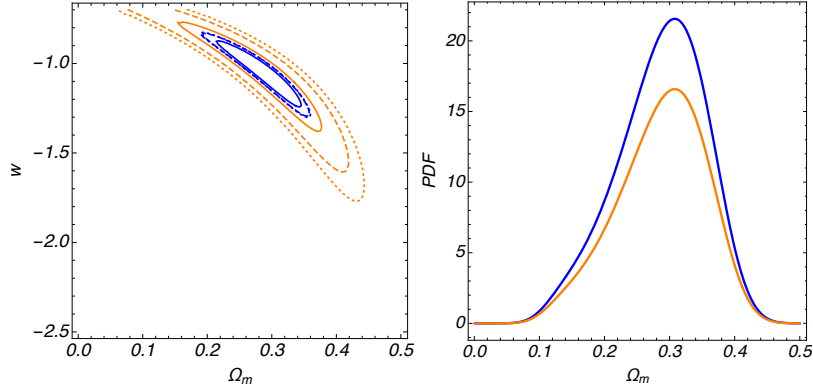


FIG. 2: General Taylor Expansion model contours plots for Cases 1.1 (orange color) and 1.2 (blue color) using CC+Pantheon+BAO samplers.

- Case 2.1: Solving the system Eqs.(15)-(16) with the condition that $T < B$, i.e we have domination of the boundary term over the torsion scalar. Also we consider $A_{i+1} > A_i$.
- Case 2.2: Solving the system Eqs.(15)-(16) with the condition that $T > B$, i.e we have domination of the torsion scalar over the boundary term). Also we consider $A_{i+1} < A_i$.

Following the above scenarios (cf. with Figure 1), we notice that in both Cases 1.1 and 1.2 (cf. with Figure 1 - *left*) the General Taylor Expansion EoS mimic the same evolution at high redshifts, which indicates that at early times the boundary term and the torsion scalar are indistinguishable if we consider the influence of an X -fluid. On the other hand, at $z \approx 1$ ⁴ a scenario where the boundary scalar dominate we have a quintessence-like behaviour that approaches more to a Λ CDM EoS than the scenario where the torsion scalar dominates. Cases 2.1 and 2.2 (cf. with Figure 1 - *middle* and *right*) show a divergence due the degeneracies of the constants A_i .

For the model given in Eq.(51), we perform the fitting using the completed compilation of data samplers described in §. IV. This analysis is showed in Figure 2, where we notice that the model has a preference for a phantom-like behaviour in agreement with Planck data value for the density of matter.

B. Power Law Model

Following Ref.[24], consider a Lagrangian of separated power law style models for the torsion and boundary scalars such that

$$f(T, B) = b_0 B^k + t_0 T^m. \quad (62)$$

⁴ Assuming a flat universe with $H_0 = 67.3 \text{ km s}^{-1} \text{ Mpc}^{-1}$, this redshift correspond to a look-back time of 7.95 Gyr.

All the derivatives corresponding to f_T and f_B functions for this model can be found in the Appendix B. Since we are interested in understanding whether this power law model can reproduce a dark energy-like behaviour, we compute the EoS in Eq.(29) for the model in Eq.(62) and obtain

$$w_x(a) = -1 + \frac{\frac{b_0 6^k (k-1) k \left[\frac{a(t)\ddot{a}(t) + 2\dot{a}(t)^2}{a(t)^2} \right]^k w_{x_1} - t_0 2^{m+2} 3^m (m-1) m a(t) \left[\frac{\dot{a}(t)^2}{a(t)^2} \right]^{m+1} w_{x_2}}{3 \left\{ \frac{6[a(t)\ddot{a}(t) - \dot{a}(t)^2]}{a(t)^2} + w_{x_4} + w_{x_5} - b_0 B^k - t_0 T^m \right\}}, \quad (63)$$

where the functions w_{x_i} are given by

$$w_{x_1} = \{ (k-1)a(t)^5 \ddot{a}(t) + 48\dot{a}(t)^6 - 30a(t)\dot{a}(t)^4 \ddot{a}(t) + a(t)^4 \ddot{a}(t) [\ddot{a}(t) + 3(k-1)\dot{a}(t)] - a(t)^2 \dot{a}(t)^2 [21\ddot{a}(t)^2 + 2\ddot{a}(t)\dot{a}(t)] + a(t)^3 [3\ddot{a}(t)^3 + \dot{a}(t)(2\dot{a}(t)(\ddot{a}(t) - 2(k-1)\dot{a}(t)) - \ddot{a}(t)\ddot{a}(t))] \}, \quad (64)$$

$$w_{x_2} = [\dot{a}(t)^2 - a(t)\ddot{a}(t)] \{ \dot{a}(t)^2 - a(t) [\ddot{a}(t) + \dot{a}(t)] \}, \quad (65)$$

$$w_{x_3} = b_0 3^{k+1} (k-1) k \dot{a}(t)^3 [a(t)^2 \ddot{a}(t) - 4\dot{a}(t)^3 + 3a(t)\dot{a}(t)\ddot{a}(t)] \left[\frac{2a(t)\ddot{a}(t) + 4\dot{a}(t)^2}{a(t)^2} \right]^k, \quad (66)$$

$$w_{x_4} = \frac{t_0 2^{m+2} 3^m (m-1) m \left[\frac{\dot{a}(t)^2}{a(t)^2} \right]^m [a(t)\ddot{a}(t) - \dot{a}(t)^2] + \frac{w_{x_3}}{[a(t)\ddot{a}(t) + 2\dot{a}(t)^2]^2}}{a(t)\dot{a}(t)}, \quad (67)$$

$$w_{x_5} = \frac{b_0 6^k (k-1) k \dot{a}(t) [-a(t)^2 \ddot{a}(t) + 4\dot{a}(t)^3 - 3a(t)\dot{a}(t)\ddot{a}(t)] \left[\frac{a(t)\ddot{a}(t) + 2\dot{a}(t)^2}{a(t)^2} \right]^k}{[a(t)\ddot{a}(t) + 2\dot{a}(t)^2]^2}. \quad (68)$$

To perform the numerical analysis, we rewrite the above expression in terms of the redshift $z = a_0/a - 1$, where $z = 0$ corresponds to the present time. The power law model EoS can be expressed as

$$w(z) = -1 + \frac{b_0 3^k 8^{k-2} (k-1) k (z+1)^{12} \left[\frac{1}{(z+1)^2} \right]^k w(z)_1 - t_0 2^{m+2} 3^m (m-1) m (z+1)^5 w(z)_2 \left[\frac{1}{(z+1)^2} \right]^{m+1}}{3 \left\{ -b_0 B^k - (z+1)^3 w(z)_3 - b_0 2^{3k-1} 3^k (k-1) k \left[\frac{1}{(z+1)^2} \right]^k - t_0 T^m + \frac{6}{(z+1)^2} \right\}}, \quad (69)$$

where

$$w(z)_1 = \left\{ -\frac{6(k-1)}{(z+1)^9} + \frac{2 \left[\frac{24}{(z+1)^5} - \frac{3(k-1)}{(z+1)^2} \right]}{(z+1)^7} + \frac{\frac{24}{(z+1)^9} - \frac{\frac{12}{(z+1)^7} - \frac{2 \left[\frac{2(k-1)}{(z+1)^2} + \frac{24}{(z+1)^5} \right]}{(z+1)^2}}{(z+1)^3} - \frac{108}{(z+1)^{12}} \right\}, \quad (70)$$

$$w(z)_2 = \left[\frac{1}{(z+1)^4} - \frac{\frac{2}{(z+1)^3} - \frac{1}{(z+1)^2}}{z+1} \right], \quad (71)$$

$$w(z)_3 = \left\{ \frac{b_0 2^{3k-1} 3^{k+1} (k-1) k \left[\frac{1}{(z+1)^2} \right]^k}{(z+1)^4} + \frac{t_0 2^{m+2} 3^m (m-1) m \left[\frac{1}{(z+1)^2} \right]^m}{(z+1)^4} \right\}. \quad (72)$$

Notice that Eq.(69) reduces to the standard Λ CDM model $w = -1$ when $f(T, B) = 0$, as expected. As a first strategy, we are going to analyse the behaviour of the EoS in Eq.(69) which is associated with the X -fluid considering seven cases (c.f. Figure 3)

- Case 1.1: Solving the system Eqs.(15)-(16) with the condition that $T < B$, i.e we have domination of the boundary term over the torsion scalar.
- Case 1.2: Solving the system Eqs.(15)-(16) with the condition that $T > B$, i.e we have domination of the torsion scalar over the boundary term)

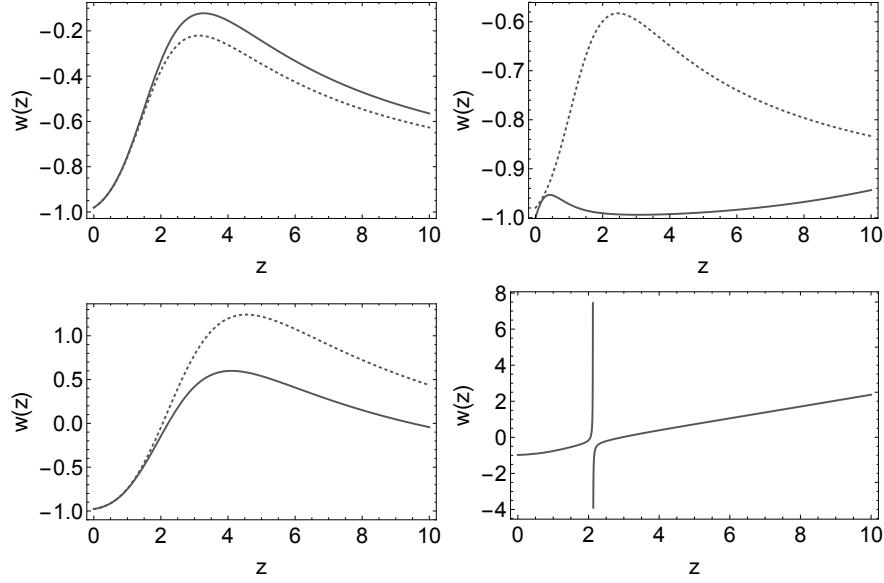


FIG. 3: Evolution of Power Law EoS (69). *Top Left*: Case 1: solving T and B , with $T < B$ (solid line) and $T > B$ (dashed line). *Top Right*: Case 2: Varying m and k , with $m < k$ (solid line) and $m > k$ (dashed line). *Bottom Left*: Case 3: Varying b_0 and t_0 , with b_0 negative and f_0 positive (solid line) and viceversa (dashed line). *Bottom Right*: Case 4: varying t_0 and m as negative values.

Parameters	Best-fit	Mean $\pm\sigma$	95% lower	95% upper
H_0	67.74	$67.74^{+1.1}_{-1.1}$	65.54	69.89
m	78.93	$79.19^{+4}_{-6.1}$	70.17	88.64
k	49.62	$49.81^{+0.73}_{-1}$	47.82	51.73
b_0	$8.16e+15$	$1.099e+16^{+7e+14}_{-1.1e+16}$	$9.981e+11$	$1.640e+15$
c_0	$8.949e+15$	$7.974e+15^{+2.8e+15}_{-6.3e+15}$	$1.169e+16$	$1.074e+16$

TABLE II: Parameters and mean values for the Power law model.

- Case 2.1: varying m and k with the condition that $m > k$.
- Case 2.2: varying m and k with the condition that $k > m$.
- Case 3.1: varying b_0 and t_0 with the condition that $b_0 < t_0$.
- Case 3.2: varying b_0 and t_0 with the condition that $b_0 > t_0$.
- Case 4: varying t_0 and m as negative values.

Following the results explored, we notice that Cases 1.1 and 1.2 (cf. with Figure 3 - top left) at $z < 2$ show an accelerating cosmic expansion, while after this point Case 1.1 starts to decelerate at $z = 3$, meanwhile Case 1.2 still preserves this acceleration with EoS $w < -1/3$. Cases 2.1 and 2.2 (cf. with Figure 3 - top right) have an EoS with $w < -1/3$, but the latter shows an asymptotic behaviour to Λ CDM between $z = 2$ and $z = 4$, which then starts to grow asymptotically to the first model at large redshift. Both Cases 3.1 and 3.2 cross the phantom divided-line, below $z = 2$ they are indistinguishable. Below $z = 2.5$ both models can start with an EoS with $w < -1/3$, where both have an asymptotic behaviour at large redshifts which can mimic a matter phase with $w = 0$ (cf. with Figure 3 - bottom left).

This is a case of an oscillating X -fluid EoS below $z = 6$. Case 4 (cf. with Figure 3 - bottom right) has an oscillating particularity, but it experiences a divergence point due to the corresponding energy-density becoming zero.

For the model given by Eq.(69), we perform the fitted using the completed compilation of data samplers described in §. IV.

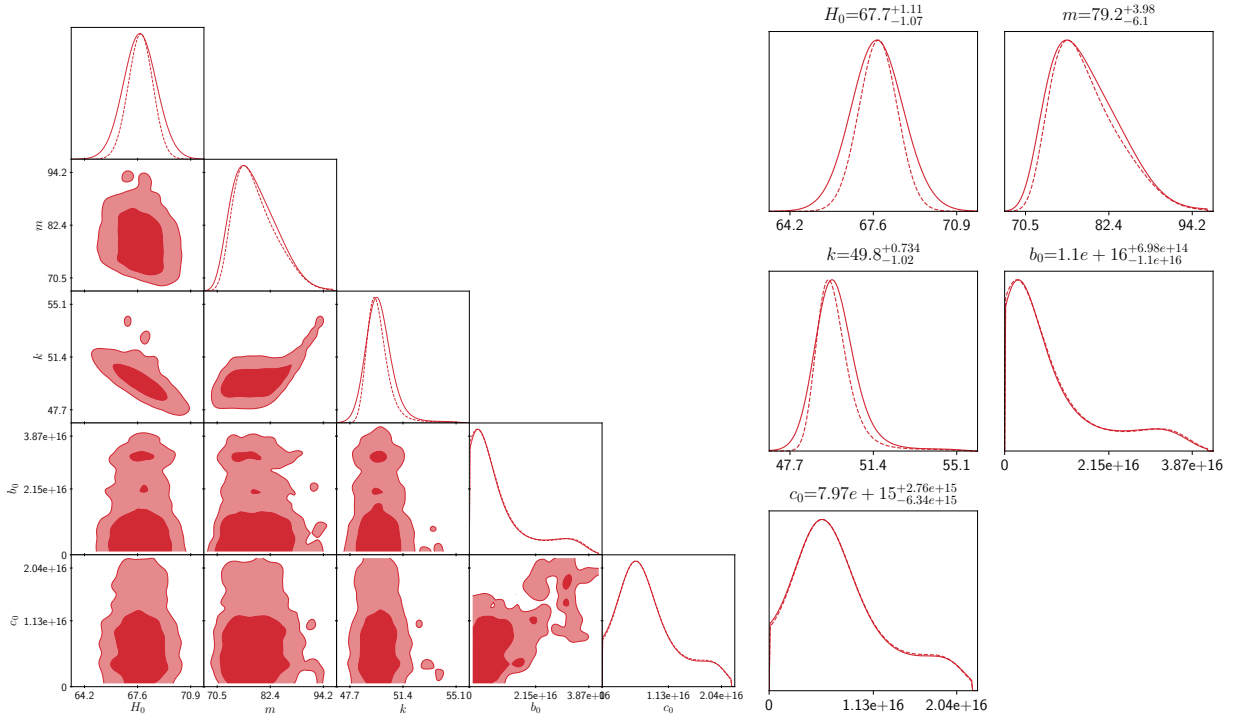


FIG. 4: One-dimensional marginalised distribution, and two-dimensional contours with 68% and 95% confidence level for the free parameters of the Power Law model using the constrained solutions for T and B scalars and CC+Pantheon+BAO total sampler.

C. Mixed Power Law Model

In Ref.[24], it was shown that this model can reproduce several important power law scale factors relevant for several cosmological epochs. This models takes the form

$$f(T, B) = f_0 B^k T^m, \quad (73)$$

where the second and fourth order contributions will now be mixed, and f_0, k, m are arbitrary constants. All the derivatives corresponding to f_T and f_B functions for this model can be found in the Appendix C.

As in the latter scenarios, we can compute the EoS in Eq.(29) for the model in Eq.(73), obtaining

$$w_x(a) = \frac{w_{x_1} a(t)^6 + 6w_{x_2} a(t)^5 + 576w_{x_3} \dot{a}(t)^6 + 24w_{x_4} a(t) \dot{a}(t)^4 + 12w_{x_5} a(t)^3 \dot{a}(t) - 6w_{x_6} a(t)^4 + 12w_{x_7} a(t)^2 \dot{a}(t)^2}{Ba(t) [72\dot{a}(t)^5 w_{x_8} - 36\dot{a}(t)^3 a(t) w_{x_9} + 36a(t)^2 \dot{a}(t)^2 w_{x_{10}} + a(t)^5 w_{x_{11}}]}, \quad (74)$$

where, for this case, the functions w_{x_i} are given by

$$w_{x_1} = -T^{m+2} f_0 B^{k+3}, \quad (75)$$

$$w_{x_2} = \left(B^2 T^2 a''(t) - 2B^k (k-1) k T^m f_0 \left(a^{(4)}(t) T^2 + (m-1) a^{(3)}(t) \right) \right) B, \quad (76)$$

$$w_{x_3} = kT \left(B^k (-(k-1)(B+2k-4) - B(k-2)m) T^m - B^3 m T \right) f_0, \quad (77)$$

$$w_{x_4} = f_0 \left(T^m (4(m-1)mB^3 - (8B+9)kmTB - 18(k-1)kT^2) a'(t) B^{k+1} \right. \\ \left. + 6kT ((k-1)(7B+12k-24) + 7B(k-2)m) T^m B^k + 7mTB^3 \right) a''(t), \quad (78)$$

$$w_{x_5} = f_0 \left(T^m (2B(k(m-1)(2k+Bm-2)a'(t)^2 + (-2(m-1)mB^3 + 3kmTB^2 + 9(k-1)kT^2) a''(t)a'(t) \right. \\ \left. + B^2 m(-2mB+2B+3kT)a''(t)^2) + kT (B(4mB^2 + 9(k-1)T) a'(t) - 12((k-1)(B+3k-6) \right. \\ \left. + B(k-2)m)a''(t)) a^{(3)}(t) B^k + 2kmT^2 a''(t) (5Ba'(t) - 6a^{(3)}(t)) B^3 \right), \quad (79)$$

$$w_{x_6} = 2kT^m f_0 \left(6(k-2)(k-1)Ta^{(3)}(t)^2 - 2BT(ma''(t)B^2 + (mB^2 - kT + T) a'(t)) a^{(3)}(t) \right. \\ \left. + Ba''(t) (3(k-1)a''(t)T^2 + (m-1)(3k+2Bm-3)a'(t)) B^k \right. \\ \left. + T^2 (a'(t)^2 + 4Bkmf_0 a^{(3)}(t)a'(t) + 4Bkmf_0 a''(t)^2) B^3 \right), \quad (80)$$

$$w_{x_7} = f_0 \left(B^k T^m (4B((m-1)mB^3 - 2kmTB^2 - 3(k-1)kT^2) a'(t)^2 \right. \\ \left. + [B(-4(m-1)mB^3 + 2(2B+9)kmTB + 27(k-1)kT^2) a''(t) \right. \\ \left. + 12k((k-1)(B+4k-8) + B(k-2)m)Ta^{(3)}(t)) \right. \\ \left. \times a'(t) - 18k((k-1)(2B+3k-6) + 2B(k-2)m)Ta''(t)^2) \right. \\ \left. - 6B^3 kmT^2 (Ba'(t)^2 - 2a^{(3)}(t)a'(t) + 6a''(t)^2) \right], \quad (81)$$

$$w_{x_8} = T^m (-2(m-1)mB^3 + (4B+3)kmTB + 6(k-1)kT^2) f_0 B^k, \quad (82)$$

$$w_{x_9} = T^m f_0 \left(2kT(Bm + 2(k-1)T)a'(t) \right. \\ \left. + (-4(m-1)mB^3 + 6(B+1)kmTB + 9(k-1)kT^2) a''(t) \right) B^k, \quad (83)$$

$$w_{x_{10}} = kT^{m+1} f_0 \left((2Bm + 3(k-1)T)a''(t) + (-2mB^2 - 3kT + 3T) a^{(3)}(t) \right) B^k, \quad (84)$$

$$w_{x_{11}} = T^{m+2} f_0 B^{k+2} - 6T^2 a(t)^4 a''(t) B^2 + 6T^2 a(t)^3 a'(t) \left(6(k-1)kT^m f_0 a^{(3)}(t) B^k + a'(t) B^2 \right), \quad (85)$$

Again, we rewrite the above expression in terms of the redshift $z = a_0/a - 1$, therefore the mixed power law model EoS can be expressed as

$$w(z) = \frac{(z+1) [w(z)_1 + w(z)_2 + 24w(z)_3 + 12w(z)_4 - 12w(z)_5 + 576w(z)_6 - 6w(z)_7]}{B [w(z)_8 + 36w(z)_9 - w(z)_{10} + w(z)_{11}]}, \quad (86)$$

where

$$w(z)_1 = -\frac{T^{m+2}f_0B^{k+3}}{(z+1)^6}, \quad (87)$$

$$w(z)_2 = \frac{6\left(\frac{2B^2T^2}{(z+1)^3} - 2B^k(k-1)kT^m\left(\frac{24T^2}{(z+1)^5} - \frac{6(m-1)}{(z+1)^4}\right)f_0\right)B}{(z+1)^5}, \quad (88)$$

$$(z+1)^9f_0w(z)_3 = \frac{12kT\left(((k-1)(7B+12k-24)+7B(k-2)m)T^mB^k+7mTB^3\right)}{(z+1)^3} - \frac{B^{k+1}T^m\left(4(m-1)mB^3-(8B+9)kmTB-18(k-1)kT^2\right)}{(z+1)^2}, \quad (89)$$

$$(z+1)^6w(z)_4 = B^kT^m\left(-\frac{72k((k-1)(2B+3k-6)+2B(k-2)m)T}{(z+1)^6} - w(z)_{12} + w(z)_{13}\right) - 6B^3kmT^2\left(\frac{B}{(z+1)^4} + \frac{12}{(z+1)^6}\right)f_0, \quad (90)$$

$$w(z)_5 = \frac{T^mw(z)_{14}B^k + \frac{4kmT^2\left(\frac{36}{(z+1)^4} - \frac{5B}{(z+1)^2}\right)B^3}{(z+1)^3}f_0}{(z+1)^5}, \quad (91)$$

$$w(z)_6 = \frac{kT\left(B^k((1-k)(B+2k-4)-B(k-2)m)T^m - B^3mT\right)f_0}{(z+1)^{12}}, \quad (92)$$

$$(z+1)^4w(z)_7 = 2kT^m\left(w(z)_{15} + \frac{216(k-2)(k-1)T}{(z+1)^8} + \frac{2B\left[\frac{6(k-1)T^2}{(z+1)^3} - \frac{(m-1)(3k+2Bm-3)}{(z+1)^2}\right]}{(z+1)^3}\right)f_0B^k + T^2\left(\frac{40Bkmf_0}{(z+1)^6} + \frac{1}{(z+1)^4}\right)B^3, \quad (93)$$

$$w(z)_8 = \frac{36kT^{m+1}\left[\frac{2(2Bm+3(k-1)T)}{(z+1)^3} - \frac{6(-2mB^2-3kT+3T)}{(z+1)^4}\right]f_0B^k}{(z+1)^6}, \quad (94)$$

$$w(z)_9 = \frac{T^m\left[\frac{2(-4(m-1)mB^3+6(B+1)kmTB+9(k-1)kT^2)}{(z+1)^3} - \frac{2kT(Bm+2(k-1)T)}{(z+1)^2}\right]f_0B^k}{(z+1)^7}, \quad (95)$$

$$w(z)_{10} = \frac{72T^m(-2(m-1)mB^3+(4B+3)kmTB+6(k-1)kT^2)f_0B^k}{(z+1)^{10}}, \quad (96)$$

$$w(z)_{11} = \frac{T^{m+2}f_0B^{k+2}}{(z+1)^5} - \frac{12T^2B^2}{(z+1)^7} - \frac{6T^2\left(-\frac{36(k-1)kT^mf_0B^k}{(z+1)^4} - \frac{B^2}{(z+1)^2}\right)}{(z+1)^5}, \quad (97)$$

$$w(z)_{12} = \frac{\frac{2B(-4(m-1)mB^3+2(2B+9)kmTB+27(k-1)kT^2)}{(z+1)^3} - \frac{72k((k-1)(B+4k-8)+B(k-2)m)T}{(z+1)^4}}{(z+1)^2}, \quad (98)$$

$$w(z)_{13} = \frac{4B[(m-1)mB^3-2kmTB^2-3(k-1)kT^2]}{(z+1)^4}, \quad (99)$$

$$w(z)_{14} = 2B\left(\frac{4m(-2mB+2B+3kT)B^2}{(z+1)^6} + \frac{k(m-1)(2k+Bm-2)}{(z+1)^4} - \frac{2(-2(m-1)mB^3+3kmTB^2+9(k-1)kT^2)}{(z+1)^5}\right) - \frac{6kT\left(-\frac{24((k-1)(B+3k-6)+B(k-2)m)}{(z+1)^3} - \frac{B(4mB^2+9(k-1)T)}{(z+1)^2}\right)}{(z+1)^4}, \quad (100)$$

$$w(z)_{15} = \frac{12B\left[\frac{2B^2m}{(z+1)^3} - \frac{mB^2-kT+T}{(z+1)^2}\right]T}{(z+1)^4}, \quad (101)$$

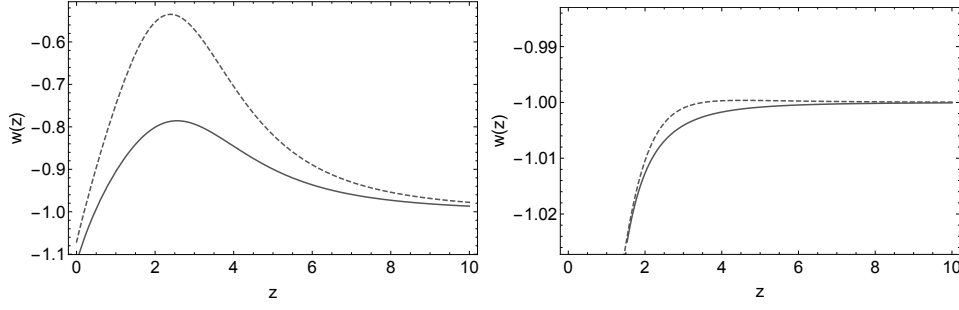


FIG. 5: Evolution of Mixed Power Law EoS (86). *Left*: Case 1: resolving T and B , with $T < B$ (solid line) and $T > B$ (dashed line). *Right*: Case 2: Varying m and k , with $m < k$ (solid line) and $m > k$ (dashed line).

Parameter	best-fit	mean $\pm\sigma$	95% lower	95% upper
H_0	67.92	$67.86^{+1.2}_{-1.1}$	65.63	70.1
m	36.59	$38.02^{+2.1}_{-2.6}$	33.71	42.45
k	2.55	$2.626^{+0.11}_{-0.13}$	2.396	2.861
c_0	$1.653e+11$	$4.97e+11^{+2.6e+11}_{-5e+11}$	$2.353e+09$	$4.847e+09$

TABLE III: Parameters and mean values for the Mixed Power Law Model model.

Analysing the behaviour of the EoS in Eq.(86) which is associated with the X -fluid considering X cases (c.f. Figure 5) and with f_0 as a positive constant

- Case 1.1: Resolving the system Eqs.(15)-(16) with the condition that $T < B$, i.e we have domination of the boundary term over the torsion scalar.
- Case 1.2: Resolving the system Eqs.(15)-(16) with the condition that $T > B$, i.e we have domination of the torsion scalar over the boundary term)
- Case 2.1: varying m and k with the condition that $m > k$.
- Case 2.2: varying m and k with the condition that $k > m$.

As in Cases 1 and 2 of the Power Law model, the Cases 1.1 and 1.2 (cf. with Figure 5 - left) in this model cross the phantom divided-line but preserve its quintessence behaviour until at high redshift both scenarios limiting to Λ CDM model. For the Cases 2 (cf. with Figure 5 - right), at $z < 4$ both scenarios mimic a phantom energy.

For the model given by Eq.(86), we perform the fitted using the completed compilation of data samplers described in §. IV.

D. Boundary Term Deviations to TEGR model

In general, we can embody modifications to TEGR as

$$f(T, B) = -T + g(B), \quad (102)$$

where modifications to standard gravity are chosen to be expressed through contributions from the boundary term only. One interesting model also investigated in Ref.[24] is the one where

$$g(B) = f_1 B \ln B, \quad (103)$$

where f_1 is an arbitrary constant.

As in the latter scenarios, we can compute the EoS (29) for (102) and obtain

$$w_x(a) = \frac{1152f_1\dot{a}(t)^6 + 6Ba(t)^5w_{x_1} + w_{x_8} - 36f_1a(t)^2\dot{a}(t)^2w_{x_5} + B^2a(t)^6(T - Bf_1\ln B)}{Ba(t)[w_{x_6} - 36w_{x_7} + Ba(t)^5(Bf_1\ln B - T)]}, \quad (104)$$

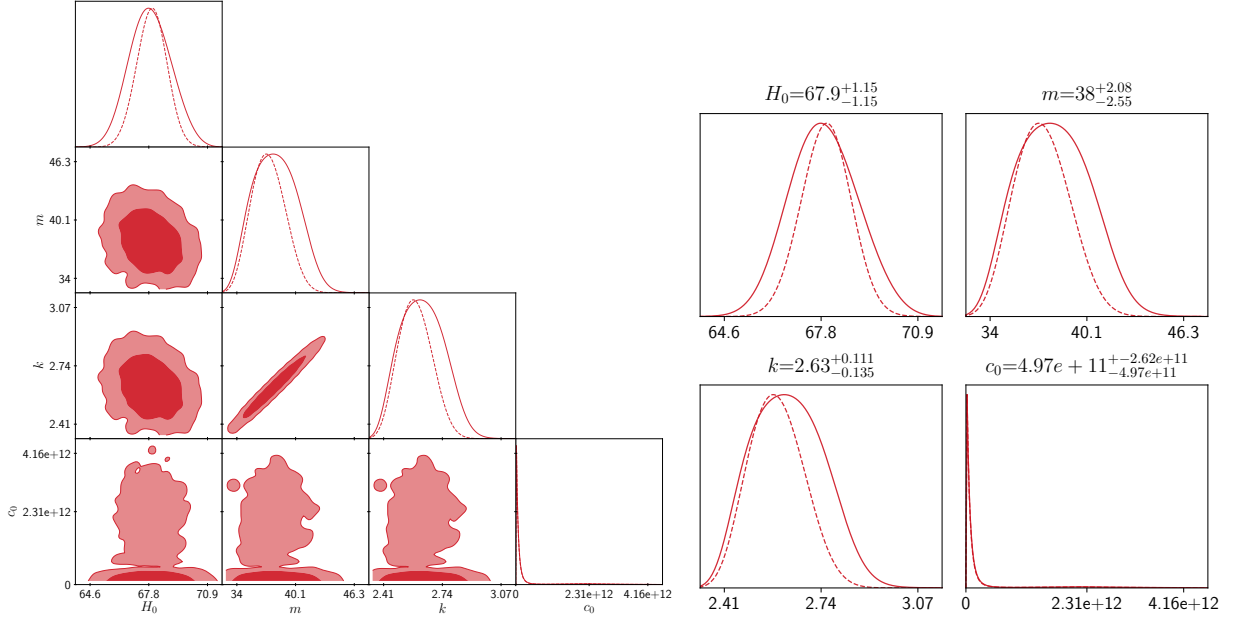


FIG. 6: One-dimensional marginalised distribution, and two-dimensional contours with 68% and 95% confidence level for the free parameters for the Mixed Power Law model using the constrained solutions for T and B scalars and CC+Pantheon+BAO total sampler.

where

$$w_{x_1} = B\ddot{a}(t) - 2f_1a^{(4)}(t), \quad (105)$$

$$w_{x_2} = 4\ddot{a}(t) + B\dot{a}(t), \quad (106)$$

$$w_{x_3} = B^2\dot{a}(t)^2 + 6f_1 \left[B\ddot{a}(t)^2 - 2a^{(3)}(t)^2 \right] + 4Bf_1a^{(3)}(t), \quad (107)$$

$$w_{x_4} = 4a^{(3)}(t)\ddot{a}(t) + Ba'(t) \left[a^{(3)}(t) + 2\ddot{a}(t) \right], \quad (108)$$

$$w_{x_5} = -18\ddot{a}(t)^2 + 4B\dot{a}(t)^2 + \dot{a}(t) \left[16a^{(3)}(t) - 9B\ddot{a}(t) \right], \quad (109)$$

$$w_{x_6} = -6Ba(t)^4\ddot{a}(t) + 432f_1\dot{a}(t)^5 + 6a(t)^3\dot{a}(t) \left[6f_1a^{(3)}(t) + B\dot{a}(t) \right], \quad (110)$$

$$w_{x_7} = f_1a(t)\dot{a}(t)^3 \left[9\ddot{a}(t) + 4\dot{a}(t) \right] + 108f_1a(t)^2\dot{a}(t)^2 \left[\ddot{a}(t) - a^{(3)}(t) \right], \quad (111)$$

$$w_{x_8} = -432f_1a(t)\dot{a}(t)^4w_{x_2} - 6a(t)^4w_{x_3} + 108f_1a(t)^3\dot{a}(t)w_{x_4}, \quad (112)$$

We rewrite the above expression in terms of the redshift $z = a_0/a - 1$, which leads to the mixed power law model EoS being expressed as

$$w(z) = \frac{B^2(z+1)^4 \left[T(z+1)^2 + 6 \right] - f_1 \left[B^3(z+1)^6 \ln B + 288(B(z+1)(z+4) - 16) \right]}{B(z+1) \left[f_1 (B^2(z+1)^5 \ln B + 288(z+4)) - B(z+1)^3 (T(z+1)^2 + 6) \right]}. \quad (113)$$

As we can see from Eq.(103), we need the existence of the boundary scalar with a constraint equation given by $3H^2 + \dot{H} = 1/6$ (for $N=1$) and $f_1 > 0.1$ in order to avoid singularities on the EoS in Eq.(113). The behaviour for this case is show in Figure 7, where we notice that when the boundary scalar dominates over the torsion scalar its EoS mimics a quintessence fluid, while on the contrary, we notice solely a phantom behaviour. Both scenarios limiting to a Λ CDM model at larger redshifts.

For the model given by (113), we perform the fitted using the completed compilation of data samplers described in §. IV.

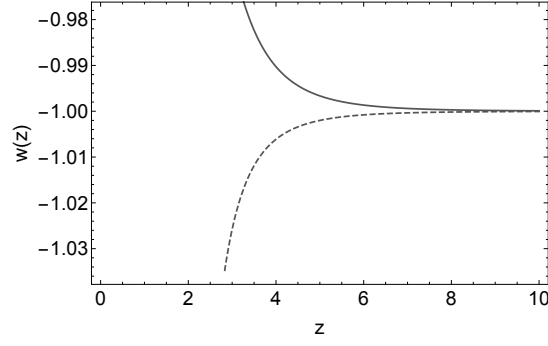


FIG. 7: Evolution of TEGR EoS (113). Here we solved T and B , with $T < B$ (solid line) and $T > B$ (dashed line).

Parameter	best-fit	mean $\pm\sigma$	95% lower	95% upper
H_0	79.77	$79.83^{+0.9}_{-0.91}$	78.03	81.64
f_1	0.203	$0.203^{+0.002}_{-0.002}$	0.199	0.208

TABLE IV: Parameters and mean values for the TEGR Deviations model.

VI. CONCLUSIONS

In this paper we presented cosmological analyses for $f(T, B)$ theory with a flat homogeneous and isotropic metric. Also, we obtained a generic equation of state w_{eff} (29) from which we can consider any cosmological form for the torsion scalar and boundary terms. As a first approach, we proposed four $f(T, B)$ cosmological scenarios where we obtained:

1. The analytical solutions for the $w(z)$ for each model and,
2. full data analyses, where we were capable to constrain the free cosmological parameters for our models using a total sampler of CC+PantheonSNeIa+BAO, fitted with Planck 2018 and SH0ES+H0LiCOW, respectively.

The main results for these cosmological models are:

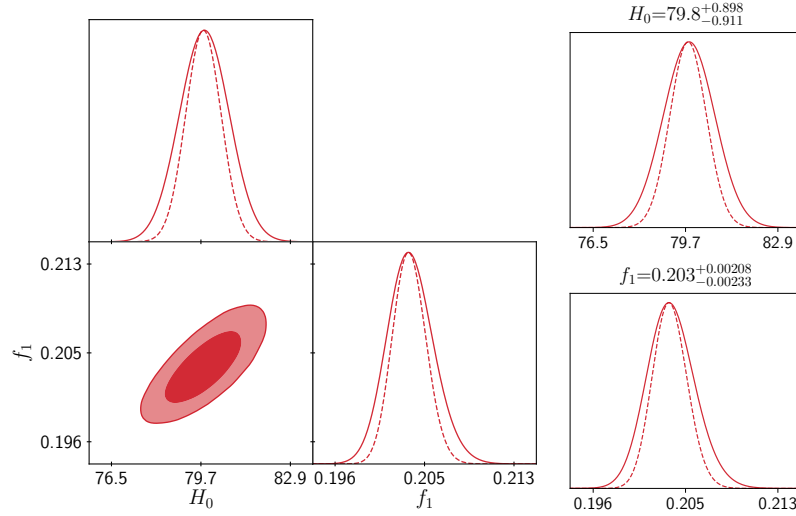


FIG. 8: One-dimensional marginalised distribution, and two-dimensional contours with 68% and 95% confidence level for the free parameters for TEGR Deviations model contours using the constrained solutions for T and B scalars and CC+Pantheon+BAO total sampler.

- General Taylor Expansion Model: According to Eq.(51), where after solving the system of equations in Eqs.(15)-(16), we divided the analytical solutions in several cases: from 1.1 to 2.2. For each case it is possible to see the domination of the torsion or boundary terms. Notice that the A_i parameters need to be positive, if not we have singularities.
- Power Law Model: As in the later case, we obtained analytical solutions for Eq.(69) and divided in cases 1.2 till 4. On one hand, we notice the equation of state for this scenario reduces to the standard Λ CDM model $w = -1$ when $f(T, B) = 0$. On the other hand, this is an interesting scenario where we have an oscillating $w(z)$, but when observational samplers are used, this model wants to remain phantom-like. This scenario seems to be in agreement with the value H_0 given by Planck 2018 with a difference of $0.3\text{-}\sigma$, c.f. with Figure 4.
- Mixed Power Law Model: For this scenario we have Cases 1.1 till 2.2. It can reproduce Λ CDM at high redshifts. This scenario, as the latter, seems to be in agreement with the value of H_0 given by Planck 2018 with a difference of $0.5\text{-}\sigma$, but c_0 is quite correlated with H_0 , c.f. with Figure 6.
- Boundary Term Deviations to TEGR model: We can recover again Λ CDM for two cases. The value of the free parameter f_1 seems to remain small with the entire sampler used. Even more, there is an intriguing result: the H_0 value is greater than the reported by SH0ES+H0LiCOW, even higher than the one using SBF calibrations [57].

All these results lead us to believe that an extension as $f(T, B)$ Teleparallel Gravity can be a good scenario, where we can consider that the role of torsion and boundary terms, fitted with astrophysical data, can shed light in the study of the late-time accelerating Universe. According to our data analyses, this theoretical direction can be an accurate expansion of the standard cosmological model to merit further research in order to pursue a fit more precise from widely different cosmic epochs, e.g for early universe, study that we will report elsewhere.

Acknowledgments

CE-R is supported by the Royal Astronomical Society as FRAS 10147. The authors thankfully acknowledge computer resources and support provided by C. Nahmad and TOCHTLI-ICN-UNAM cluster. This article is based upon work from CANTATA COST (European Cooperation in Science and Technology) action CA15117, EU Framework Programme Horizon 2020.

Appendix A: Derivation for the General Taylor Expansion model

For this model, the Lagrangian turns out to be

$$f(T, B) \simeq A_0 + A_1 T + A_2 T^2 + A_3 B^2 + A_4 T B, \quad (\text{A1})$$

where if we use Eqs.(15)-(16), the EoS in Eq.(29) can be related to the Hubble (or scale) factor directly. These derivatives are given by

$$f_T = A_1 + 2A_2 T + A_4 B, \quad (\text{A2})$$

$$\dot{f}_T = 24A_2 H \dot{H} + 6A_4 (6H \dot{H} + \ddot{H}), \quad (\text{A3})$$

$$f_B = 2A_3 B + A_4 T, \quad (\text{A4})$$

$$\dot{f}_B = 12A_3 (6H \dot{H} + \ddot{H}) + 12A_4 H \dot{H}, \quad (\text{A5})$$

$$\ddot{f}_B = 12A_3 (6\dot{H}^2 + 6H\ddot{H} + \ddot{H}) + 12A_4 (\dot{H}^2 + H\ddot{H}), \quad (\text{A6})$$

where the torsion scalar and boundary term represent the quantities in Eq.(15) and Eq.(16) respectively.

Appendix B: Derivation for the Power Law model

For this model, the Lagrangian turns out to be

$$f(T, B) = b_0 B^k + t_0 T^m, \quad (\text{B1})$$

where the contributing elements to the EoS parameter in Eq.(29) are given by

$$f_T = t_0 m T^{m-1}, \quad (\text{B2})$$

$$\dot{f}_T = 12 t_0 m (m-1) H \dot{H} (6H^2)^{m-2}, \quad (\text{B3})$$

$$f_B = b_0 k B^{k-1}, \quad (\text{B4})$$

$$\dot{f}_B = 6 b_0 k (k-1) \left[6(3H^2 + \dot{H}) \right]^{k-2} (6H\dot{H} + \ddot{H}), \quad (\text{B5})$$

$$\ddot{f}_B = 6 b_0 k (k-1) \left[6(3H^2 + \dot{H}) \right]^{k-2} \left\{ \frac{k-1}{3H^2 + \dot{H}} (6H\dot{H} + \ddot{H}) + 6\dot{H}^2 + 6H\ddot{H} + \ddot{H} \right\}, \quad (\text{B6})$$

where it can be seen that the torsion scalar embodies the second order elements of the $f(R)$ gravity while the boundary term B takes on its fourth order contributions.

Appendix C: Derivation for the Mixed Power Law Model

This models takes the form

$$f(T, B) = f_0 B^k T^m, \quad (\text{C1})$$

where the second and fourth order contributions will now be mixed, and f_0, k, m are arbitrary constants. In order to compare with the Friedmann equations, consider the derivatives below

$$f_T = f_0 m B^k T^{m-1}, \quad (\text{C2})$$

$$\dot{f}_T = 6 f_0 m B^{k-1} T^{m-2} \left[k T (6H\dot{H} + \ddot{H}) + 2H\dot{H}(m-1)B \right], \quad (\text{C3})$$

$$f_B = f_0 k B^{k-1} T^m, \quad (\text{C4})$$

$$\dot{f}_B = 6 f_0 k B^{k-2} T^{m-1} \left[(k-1)(6H\dot{H} + \ddot{H})T + 2mBH\dot{H} \right], \quad (\text{C5})$$

$$\begin{aligned} \ddot{f}_B = 6 f_0 k \left\{ \left[(m-1)B^{k-2}T^{m-2} + 6(k-2)B^{k-3}T^{m-1} (6H\dot{H} + \ddot{H}) \right] \left[2mBH\dot{H} + (k-1)(6H\dot{H} + \ddot{H}) \right] \right. \\ \left. + B^{k-2}T^{m-1} \left[12H\dot{H}(k-1)(6H\dot{H} + \ddot{H}) + (k-1)T(6\dot{H}^2 + 6H\ddot{H} + \ddot{H}) \right] \right. \\ \left. + 2m(6H\dot{H}(6H\dot{H} + \ddot{H}) + B\dot{H}^2 + BH\ddot{H}) \right\}, \end{aligned} \quad (\text{C6})$$

where again the torsion scalar and boundary term represent the quantities in Eq.(15) and Eq.(16) respectively.

Appendix D: Boundary Term Deviations to TEGR model

In general, we can write the modifications to TEGR as

$$f(T, B) = -T + g(B), \quad (\text{D1})$$

with $g(B) = f_1 B \ln B$ and where f_1 is an arbitrary constant. In this circumstance, the derivative quantities in the Friedmann equations are given by

$$f_T = -1, \quad (\text{D2})$$

$$\dot{f}_T = 0, \quad (\text{D3})$$

$$f_B = f_1 \ln B + f_1, \quad (\text{D4})$$

$$\dot{f}_B = 6 f_1 \frac{6H\dot{H} + \ddot{H}}{B}, \quad (\text{D5})$$

$$\ddot{f}_B = \frac{6f_1}{B^2} \left[(6\dot{H}^2 + 6H\ddot{H} + \ddot{H}) B - 6(6H\dot{H} + \ddot{H})^2 \right]. \quad (\text{D6})$$

-
- [1] C. Misner, K. Thorne and J. Wheeler, *Gravitation*, no. pt. 3 in *Gravitation*. W. H. Freeman, 1973.
 - [2] T. Clifton, P. G. Ferreira, A. Padilla and C. Skordis, *Modified Gravity and Cosmology*, *Phys. Rept.* **513** (2012) 1 [1106.2476].
 - [3] L. Baudis, *Dark matter detection*, *J. Phys.* **G43** (2016) 044001.
 - [4] G. Bertone, D. Hooper and J. Silk, *Particle dark matter: Evidence, candidates and constraints*, *Phys. Rept.* **405** (2005) 279 [hep-ph/0404175].
 - [5] S. Weinberg, *The cosmological constant problem*, *Rev. Mod. Phys.* **61** (1989) 1.
 - [6] PLANCK collaboration, *Planck 2018 results. VI. Cosmological parameters*, **1807.06209**.
 - [7] PLANCK collaboration, *Planck 2015 results. XIII. Cosmological parameters*, *Astron. Astrophys.* **594** (2016) A13 [1502.01589].
 - [8] K. C. Wong et al., *H0LiCOW XIII. A 2.4% measurement of H_0 from lensed quasars: 5.3 σ tension between early and late-Universe probes*, **1907.04869**.
 - [9] A. Riess, “SHOES-Supernovae, H0, for the Equation of State of Dark energy.” HST Proposal, July, 2006.
 - [10] W. L. Freedman et al., *The Carnegie-Chicago Hubble Program. VIII. An Independent Determination of the Hubble Constant Based on the Tip of the Red Giant Branch*, **1907.05922**.
 - [11] L. L. Graef, M. Benetti and J. S. Alcaniz, *Primordial gravitational waves and the H0-tension problem*, *Phys. Rev.* **D99** (2019) 043519 [1809.04501].
 - [12] LIGO SCIENTIFIC, VIRGO, 1M2H, DARK ENERGY CAMERA GW-E, DES, DLT40, LAS CUMBRES OBSERVATORY, VINROUGE, MASTER collaboration, *A gravitational-wave standard siren measurement of the Hubble constant*, *Nature* **551** (2017) 85 [1710.05835].
 - [13] R. Weitzenböck, ‘*Invariantentheorie*’. Noordhoff, Gronningen, 1923.
 - [14] R. Aldrovandi and J. G. Pereira, *Teleparallel Gravity*, vol. 173. Springer, Dordrecht, 2013, **10.1007/978-94-007-5143-9**.
 - [15] D. Blixt, M. Hohmann and C. Pfeifer, *Hamiltonian and primary constraints of new general relativity*, *Phys. Rev.* **D99** (2019) 084025 [1811.11137].
 - [16] D. Blixt, M. Hohmann and C. Pfeifer, *On the gauge fixing in the Hamiltonian analysis of general teleparallel theories*, *Universe* **5** (2019) 143 [1905.01048].
 - [17] Y.-F. Cai, S. Capozziello, M. De Laurentis and E. N. Saridakis, *$f(T)$ teleparallel gravity and cosmology*, *Rept. Prog. Phys.* **79** (2016) 106901 [1511.07586].
 - [18] R. Aldrovandi, J. G. Pereira and K. H. Vu, *Doing without the equivalence principle*, in *On recent developments in theoretical and experimental general relativity, gravitation, and relativistic field theories. Proceedings, 10th Marcel Grossmann Meeting, MG10, Rio de Janeiro, Brazil, July 20-26, 2003. Pt. A-C*, pp. 1505–1512, 2004, **gr-qc/0410042**, DOI.
 - [19] T. P. Sotiriou and V. Faraoni, *$f(R)$ Theories Of Gravity*, *Rev. Mod. Phys.* **82** (2010) 451 [0805.1726].
 - [20] V. Faraoni, *$f(R)$ gravity: Successes and challenges*, in *18th SIGRAV Conference Cosenza, Italy, September 22-25, 2008*, 2008, **0810.2602**.
 - [21] S. Capozziello and M. De Laurentis, *Extended Theories of Gravity*, *Phys. Rept.* **509** (2011) 167 [1108.6266].
 - [22] S. Bahamonde, C. G. Böhm and M. Wright, *Modified teleparallel theories of gravity*, *Phys. Rev.* **D92** (2015) 104042 [1508.05120].
 - [23] S. Capozziello, M. Capriolo and M. Transirico, *The gravitational energy-momentum pseudotensor: the cases of $f(R)$ and $f(T)$ gravity*, **1804.08530**.
 - [24] S. Bahamonde and S. Capozziello, *Noether Symmetry Approach in $f(T, B)$ teleparallel cosmology*, *Eur. Phys. J.* **C77** (2017) 107 [1612.01299].
 - [25] A. Paliathanasis, *de Sitter and Scaling solutions in a higher-order modified teleparallel theory*, *JCAP* **1708** (2017) 027 [1706.02662].
 - [26] G. Farrugia, J. L. Said, V. Gakis and E. N. Saridakis, *Gravitational Waves in Modified Teleparallel Theories*, *Phys. Rev.* **D97** (2018) 124064 [1804.07365].
 - [27] S. Bahamonde, M. Zubair and G. Abbas, *Thermodynamics and cosmological reconstruction in $f(T, B)$ gravity*, *Phys. Dark Univ.* **19** (2018) 78 [1609.08373].
 - [28] M. Wright, *Conformal transformations in modified teleparallel theories of gravity revisited*, *Phys. Rev.* **D93** (2016) 103002 [1602.05764].
 - [29] J. G. Pereira, *Teleparallelism: A New Insight Into Gravity*, in *Springer Handbook of Spacetime*, A. Ashtekar and V. Petkov, eds., pp. 197–212, Springer Berlin Heidelberg, (2014), **1302.6983**, DOI.
 - [30] S. Bahamonde, S. Capozziello, M. Faizal and R. C. Nunes, *Nonlocal Teleparallel Cosmology*, *Eur. Phys. J.* **C77** (2017) 628 [1709.02692].
 - [31] J. Beltrán Jiménez, L. Heisenberg and T. S. Koivisto, *The Geometrical Trinity of Gravity*, **1903.06830**.
 - [32] R. Aldrovandi and J. Pereira, *An Introduction to Geometrical Physics*. World Scientific, 1995.
 - [33] M. Krššák, R. J. Van Den Hoogen, J. G. Pereira, C. G. Boehmer and A. A. Coley, *Teleparallel Theories of Gravity: Illuminating a Fully Invariant Approach*, **1810.12932**.
 - [34] B. Li, T. P. Sotiriou and J. D. Barrow, *$f(T)$ gravity and local Lorentz invariance*, *Phys. Rev.* **D83** (2011) 064035 [1010.1041].
 - [35] M. Krššák and E. N. Saridakis, *The covariant formulation of $f(T)$ gravity*, *Class. Quant. Grav.* **33** (2016) 115009

- [1510.08432].
- [36] N. Tamanini and C. G. Böhrer, *Good and bad tetrads in $f(T)$ gravity*, *Phys. Rev.* **D86** (2012) 044009 [1204.4593].
 - [37] S. Bahamonde, C. G. Böhrer and M. Krššák, *New classes of modified teleparallel gravity models*, *Phys. Lett.* **B775** (2017) 37 [1706.04920].
 - [38] F. W. Hehl, P. von der Heyde, G. D. Kerlick and J. M. Nester, *General relativity with spin and torsion: Foundations and prospects*, *Rev. Mod. Phys.* **48** (1976) 393.
 - [39] V. C. de Andrade, L. C. T. Guillen and J. G. Pereira, *Gravitational energy momentum density in teleparallel gravity*, *Phys. Rev. Lett.* **84** (2000) 4533 [gr-qc/0003100].
 - [40] S. Bahamonde, *Generalised nonminimally gravity-matter coupled theory*, *Eur. Phys. J.* **C78** (2018) 326 [1709.05319].
 - [41] R. Ferraro and F. Fiorini, *Modified teleparallel gravity: Inflation without inflaton*, *Phys. Rev.* **D75** (2007) 084031 [gr-qc/0610067].
 - [42] R. Ferraro and F. Fiorini, *On Born-Infeld Gravity in Weitzenböck spacetime*, *Phys. Rev.* **D78** (2008) 124019 [0812.1981].
 - [43] G. R. Bengochea and R. Ferraro, *Dark torsion as the cosmic speed-up*, *Phys. Rev.* **D79** (2009) 124019 [0812.1205].
 - [44] E. V. Linder, *Einstein's Other Gravity and the Acceleration of the Universe*, *Phys. Rev.* **D81** (2010) 127301 [1005.3039].
 - [45] S.-H. Chen, J. B. Dent, S. Dutta and E. N. Saridakis, *Cosmological perturbations in $f(T)$ gravity*, *Phys. Rev.* **D83** (2011) 023508 [1008.1250].
 - [46] D. M. Scolnic et al., *The Complete Light-curve Sample of Spectroscopically Confirmed SNe Ia from Pan-STARRS1 and Cosmological Constraints from the Combined Pantheon Sample*, *Astrophys. J.* **859** (2018) 101 [1710.00845].
 - [47] M. Moresco, L. Pozzetti, A. Cimatti, R. Jimenez, C. Maraston, L. Verde et al., *A 6% measurement of the Hubble parameter at $z \sim 0.45$: direct evidence of the epoch of cosmic re-acceleration*, *JCAP* **1605** (2016) 014 [1601.01701].
 - [48] E. A. Kazin et al., *The WiggleZ Dark Energy Survey: improved distance measurements to $z = 1$ with reconstruction of the baryonic acoustic feature*, *Mon. Not. Roy. Astron. Soc.* **441** (2014) 3524 [1401.0358].
 - [49] F. Beutler, C. Blake, J. Koda, F. Marin, H.-J. Seo, A. J. Cuesta et al., *The BOSS-WiggleZ overlap region I. Baryon acoustic oscillations*, *Mon. Not. Roy. Astron. Soc.* **455** (2016) 3230 [1506.03900].
 - [50] F. Beutler, C. Blake, M. Colless, D. H. Jones, L. Staveley-Smith, L. Campbell et al., *The 6dF Galaxy Survey: Baryon Acoustic Oscillations and the Local Hubble Constant*, *Mon. Not. Roy. Astron. Soc.* **416** (2011) 3017 [1106.3366].
 - [51] C. Howlett, A. Ross, L. Samushia, W. Percival and M. Manera, *The clustering of the SDSS main galaxy sample - II. Mock galaxy catalogues and a measurement of the growth of structure from redshift space distortions at $z = 0.15$* , *Mon. Not. Roy. Astron. Soc.* **449** (2015) 848 [1409.3238].
 - [52] K. T. Mehta, A. J. Cuesta, X. Xu, D. J. Eisenstein and N. Padmanabhan, *A 2% Distance to $z = 0.35$ by Reconstructing Baryon Acoustic Oscillations - III : Cosmological Measurements and Interpretation*, *Mon. Not. Roy. Astron. Soc.* **427** (2012) 2168 [1202.0092].
 - [53] D. Stoppacher, F. Prada, A. D. Montero-Dorta, S. Rodriguez-Torres, A. Knebe, G. Favole et al., *A semi-analytical perspective on massive galaxies at $z \sim 0.55$* , *Mon. Not. Roy. Astron. Soc.* **486** (2019) 1316 [1902.05496].
 - [54] BOSS collaboration, *The clustering of galaxies in the completed SDSS-III Baryon Oscillation Spectroscopic Survey: cosmological analysis of the DR12 galaxy sample*, *Mon. Not. Roy. Astron. Soc.* **470** (2017) 2617 [1607.03155].
 - [55] BOSS collaboration, *Baryon acoustic oscillations in the Ly α forest of BOSS DR11 quasars*, *Astron. Astrophys.* **574** (2015) A59 [1404.1801].
 - [56] BOSS collaboration, *Quasar-Lyman α Forest Cross-Correlation from BOSS DR11 : Baryon Acoustic Oscillations*, *JCAP* **1405** (2014) 027 [1311.1767].
 - [57] L. Verde, T. Treu and A. G. Riess, *Tensions between the Early and the Late Universe*, 1907.10625.